Facile Fabrication of Light, Flexible and Multifunctional Graphene Fibers

*Zelin Dong, Changcheng Jiang, Huhu Cheng, Yang Zhao, Gaoquan Shi, Lan Jiang, and Liangti Qu**

Carbon-based fibers are of practical importance in constructing high-strength, low-weight structural materials in the transportation vehicles, civil engineering and defense. Fabrication of carbon nanotube (CNT) fibers/yarns has been attracting tremendous attentions for years with the desire to integrate such unique properties as high strength, electrical and thermal conductivities of the individual nanotubes into the useful, macroscopic ensembles. Breakthroughs have been made in wet approaches[1–4] and dry-state spinning of CNTs[5–7] for CNT fiber fabrication. CNT is the typical one dimensional (1D) nanostructure with high aspect ratio and strong binding force between its bundles.[8] As a result, just like the spinning of cotton and wool, CNT fibers and sheets can be directly drawn out from their arrays[5,7–9] or high concentration suspensions.[2–4] However, beyond the superb properties of as-produced CNT fibers, we have to face the high cost for producing the initial superaligned CNT arrays,[5,7,8] and extremely rigorous conditions such as high temperature (>1000 °C),[6] and caustic media (e.g., fuming sulfuric acid[2] and chlorosulphonic acid[4]) for CNT dispersion.

Graphene, a 2D monolayer of carbon atoms packed into a honeycomb lattice, is the basic building block for carbon materials of all other dimensionalities,[10] which gains immense recognition due to its fascinating properties such as giant electron mobility,[11–13] high thermal conductivity,[14] extraordinary elasticity and stiffness.[15] However, the lack of scalable assembly methods has been a key hurdle in manufacturing graphenes. Therefore, for integration of the remarkable properties of individual graphenes into advanced, macroscopic, functional structures for practical applications, an effective assembly strategy in a well-controlled way has to be developed. Owing to the ease of preparation and processing, as well as the scalable production and low cost, chemically derived graphene sheets hold the promise for integration into various macroscopic architectures. In virtue of the intrinsic 2D structure, graphenes have been conformably assembled into 2D macroscopic configurations such as papers,[16–18] transparent and conductive films[19,20] and even 3D frameworks.[21,22] However, it is of an extraordinary challenge to directly assemble 2D microcosmic graphene sheets into macroscopic fibers, because the irregular size and shape of chemically derived graphenes, and the movable layer-by-layer stacking of graphenes in contrary to the highly tangled CNT assembly could seriously obstruct the formation of graphene fibers and impair their macroscopic mechanical properties. As a consequence, up to date, few attempts have been successfully made to assemble graphenes into macroscopic fibers[23,24] although we are aware of the lower cost of graphene fibers than that of both CNT and commercial carbon fibers, and their practical importance for various applications.[25]

In this work, we developed a facile one-step dimensionally-confined hydrothermal strategy to fabricate the neat graphene fibers from cost-efficient aqueous graphite oxide (GO) suspensions. A glass pipeline of 0.4 mm in inner diameter was used as the reactor (Figure S1). The aqueous GO suspension of 8 mg/mL was injected into the glass pipeline, followed by baking it at 230 °C for 2 h after sealing up the two ends of the pipeline. Finally, a graphene fiber matching the pipe geometry was produced.

Figure 1a shows a 63 cm long graphene fiber with a uniform diameter of ~33 μm. 1 mL GO suspension (8 mg/mL) will generate more than 6 meter long graphene fiber. The fiber diameter and length can be controlled by either simply using the pipeline with predesigned length and inner diameter or adjusting the initial GO concentration (Figure S2 and S3). The initially formed graphene fiber released from pipeline in wet state has a relative large diameter as exemplified in Figure S4a and S5a, which has a noncompact but highly 3D cross-linking porous structure of random graphene sheets (Figure S5b,c), characteristic of the hydrothermally produced samples.[21] After being dried in air, the graphene fiber almost maintains the length (Figure S4) but its diameter has a five times reduction compared with the wet one because the water loss caused the shrinkage (Figure S5a and Movie S1). The drastic contraction in the diameter direction during the drying process could lead to the surface tension force for spontaneous orientation of graphene sheets to some extent. The capillary force during the loss of water could induce the close packing of porous graphene sheets. Consequently, the loose linkage of graphene sheets

Z. Dong,[+] C. Jiang,[+] H. Cheng, Y. Zhao, Prof. L. Qu
Key Laboratory of Cluster Science
Ministry of Education
School of Chemistry
Beijing Institute of Technology
Beijing 100081, China
E-mail: lqu@bit.edu.cn
Prof. G. Shi
Department of Chemistry
Tsinghua University
Beijing 100084, China
Prof. L. Jiang
Laser Micro-/Nano-Fabrication Laboratory
School of Mechanical Engineering
Beijing Institute of Technology
100081, China
[+] These authors contributed equally to this work.

DOI: 10.1002/adma.201200170

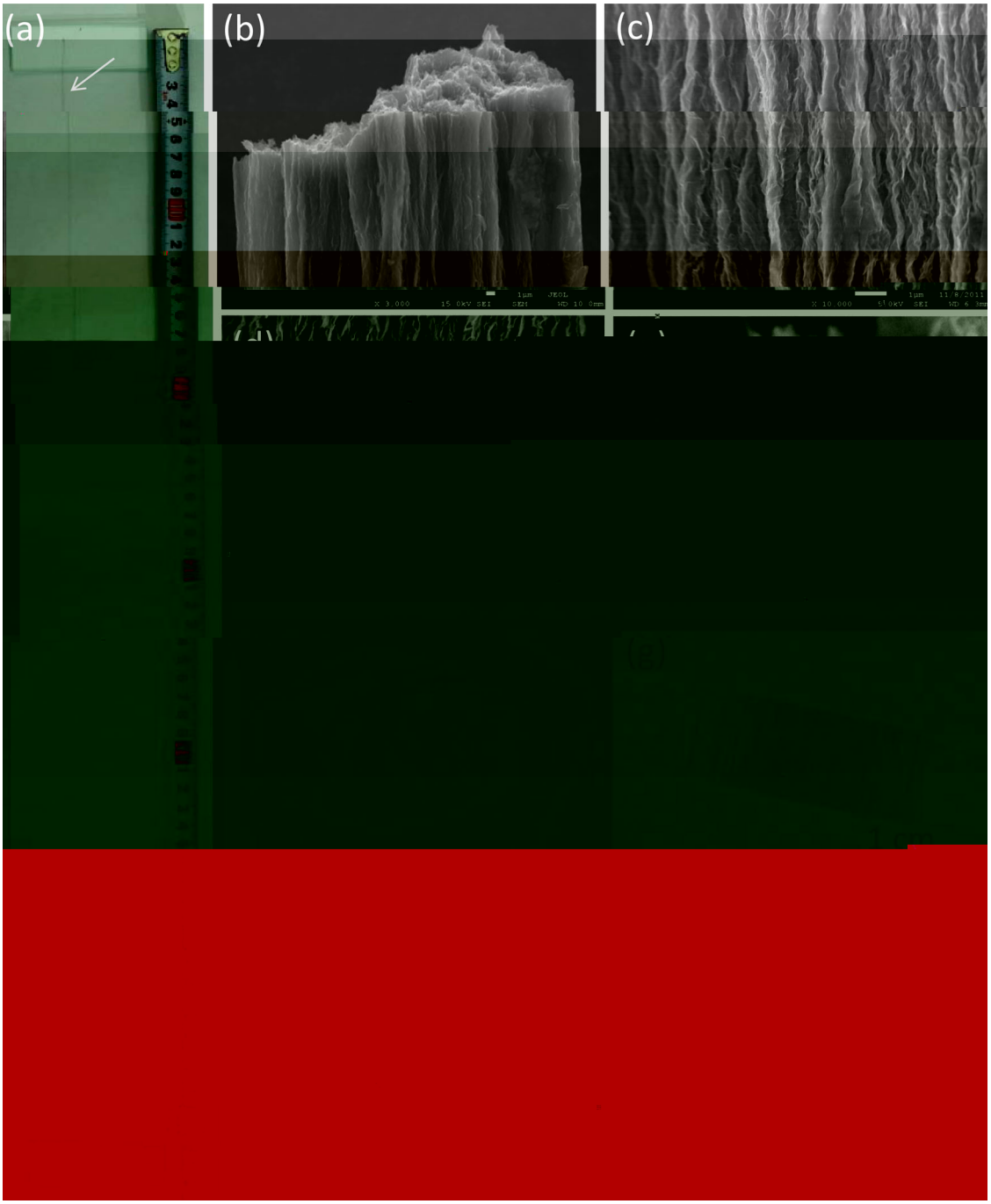

Figure 1. Morphology and flexibility of graphene fiber. (a) A photograph of a single dry graphene fiber with a diameter of ~ 33 μm and a length of 63 cm. (b) Scanning electron microscope (SEM) image of the deliberately broken part of a graphene fiber (scale bar = 1 μm). (c and d) The axial external surface and inner cross-section SEM images of graphene fiber, respectively (scale bars = 1 μm). (e) The high resolution SEM image of the broken section in (b) (scale bar = 100 nm). (f) A photograph of a wet graphene fiber coiled individually in water. (g) A photograph of dry graphene fibers coiled in bundle around the glass rod. (h and i) SEM images of the knotted and two-ply graphene fibers (scale bars = 100 μm).

becomes densely stacked and relatively aligned directionally to the fiber's main axis (Figures 1b–e and S5d&e). The broken section shows the individual graphene sheets and their compact entanglement (Figure 1e). Transmission electron microscopic (TEM) investigation and electron diffraction pattern confirm that the fiber is made out of graphene sheets (Figure S6). The alignment of graphene sheets was also evaluated by the polarized Raman spectroscopy.[2,26,27] The ratio of G-band intensity (parallel versus perpendicular) provides a useful probe of the relative degree of alignment. The neat graphene fibers possess a Raman ratio of about 6:1 (Figure S7), while the ratio is about 1:1 for the initial wet graphene fiber, indicating that the graphene

Adv. Mater. **2012**,
DOI: 10.1002/adma.201200170

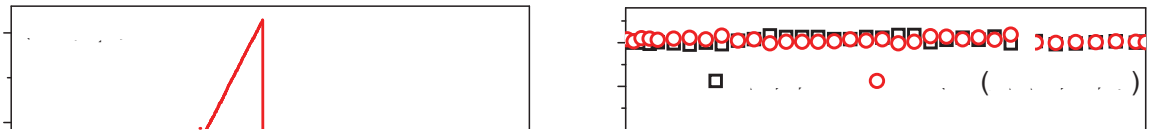

Figure 2. M electrical properties of graphene fibers. (a) Typical stress-strain curves of single as-prepared (blue square) and 800 °C thermally tr le) graphene fiber. (b) Electrical-resistance change of a graphene fiber upon repeated bending to a radius of 2 mm and then straightenin 00 cycles. The inset photographs show the straight and bending status of a graphene fiber (scale bars = 1 cm).

sheets a gned parallel to the axis of the dry fiber, which i ent with the aforementioned SEM observations. V t observed any aggregation and preformed orienta ial GO before and after being injected into the pi re S8). Therefore, the alignment of graphene sheet l to the fiber's main axis could be attributed to the e illary-induced shear force and surface tension-indu force during dry process. Just like the daily used thre aphene fiber can be curved into coils and enlaced in wet and dry states (Figures 1f,g). The fiber does no he knot is tightened (Figure 1h), and two-ply yarn ca ed by twisting two fibers (Figure 1i). These observ onstrate the flexibility and resistance to torsion of g bers, which is similar to CNT fibers.[3,6,7]

n derived from micrometer-scale GO sheets (Figure S8), thermally converted graphene fiber has a measured rength of up to 180 MPa (**Figure 2**a). This value is that of the singles yarns of multiwalled CNTs,[7] but etter than those of single-walled CNT fibers fabricated spinning process.[2–4] Higher strength of about 420 MPa rved for the graphene fibers thermally treated at 800 °C n in vacuum (Figure 2a). The dry graphene fibers have verage density of 0.23 g/cm^3, which is about 7 times r than that of carbon fibers (about 1.7–2.0 g/cm^3), and 3 times lighter than any previously reported CNT yarns g/cm^3 in ref. [7], 1.1 g/cm^3 in ref. [2]. 1.3–1.5 g/cm^3 in . [3], and 2.0 g/cm^3 in ref. [6]). As a consequence, the den-y-normalized failure stress of the graphene fibers is up to 82 MPa/g cm^{-3}, exceeding the polymer-free CNT yarns (50–75 MPa/g cm^{-3}).[2,3,6,7] The graphene fibers have typical elongations at beak of about 3 to 6%, which is comparable to that of CNT fibers,[3,7] but much larger than graphite fibers (about 1%). The elastic behavior at room temperature before break of graphene fibers presumably arises from the possible displacement of the graphene sheets within the fibers.

The hydrothermally synthesized graphene fibers have a four-probe electrical conductivity of ~10 S/cm at room temperature, which is similar to those of wet-spun single-walled CNT fibers.[3,4] We also investigated the effect of bending on the electrical resistance of graphene fiber. The bend tests were carried out with an in-house-made two-point bending device and a high-precision mechanical system. The electrical resistance remains stable and shows a negligible variation in either the bent or straight state over 1000 cycles (Figure 2b). The excellent electromechanical stability gives graphene fiber the great potential as flexible conductors for curvilinear large-area electronics such as sensory skins and wearable communication devices.[28]

The flexible and mechanically stable graphene fibers can be shaped to specific geometry on demand. The wet graphene fibers facilitate the prefabrication into various configurations, which will remain the predesigned structure once being dried. As shown in **Figure 3**a, circle, triangle and quadrangle of graphene fibers have been achieved by wrapping the wet graphene fiber around the cylindrical, triangular and quadrangular bars. The graphene fiber can even be folded into 3D architecture as exemplified by a tetrahedron in Figure 3b. A graphene fiber spring with stretchable and compressible character is also fabricated (Figure 3c–e), which shows the mechanically stable shape-memory feature.

The pliability of graphene fibers facilitates the weaving into a variety of macroscopic objects. For example, a textile structure of graphene fibers with self-supported stability was demonstrated in Figure 3f,g, which displays the great potentials in electronic-textile applications in view of the good conductivity of graphene fibers. In addition, the graphene fibers can be expediently integrated into flexible, transparent, conductive composite film. Figure 3h shows a graphene fiber network embedded into the polydimethylsiloxane (PDMS) matrix with tolerance to deformation.

Integration of functional components into the fibers will facilitate the important applications such as stimulus-responsive and electronic-textiles. The graphene fibers provide a platform for in-situ and post-synthesis incorporation of various materials with unique properties into the fiber bodies for weavable multifunctional applications. As an example, magnetic graphene fibers have been fabricated by introduction of Fe_3O_4

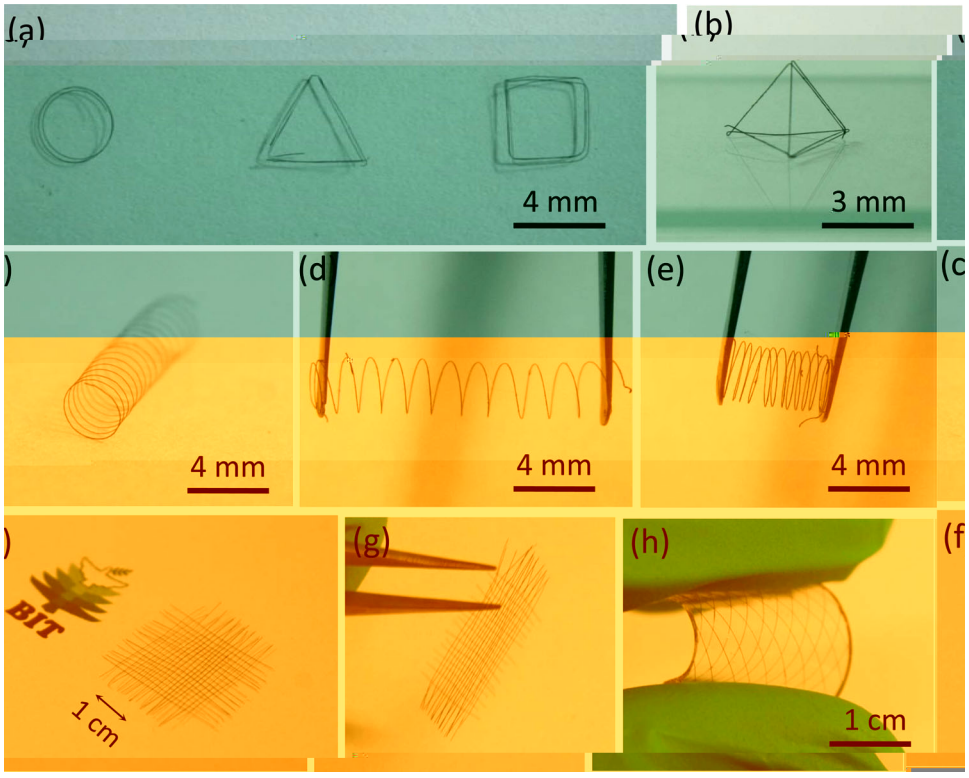

Figure 3. Shaping and weaving of graphene fibers. (a) and (b) The handmade planar and 3D geometric structures of graphene fibers, respectively. (c–e) The spring of graphene fiber at free, stretched, and compressed status, respectively. (f and g) Photographs of the hand-knitted textile of graphene fibers. (h) Photograph of graphene fiber network embedded in PDMS matrix.

nanoparticles into the fibers. The magnetic Fe_3O_4 nanoparticles were well mixed with GO suspension under ultrasonication (weight ratio of Fe_3O_4/GO = 1:10), followed by hydrothermal process within pipelines for in-situ incorporation of Fe_3O_4 into the interlayers of graphene sheets (Figure S9). The Fe_3O_4/graphene fiber with good mechanical flexibility possesses a sensitive magnetic response. As demonstrated in **Figure 4**a,b and Movies S2,S3, the magnetized graphene fiber can iteratively bend to the magnet from the initial upright position.

On the other hand, the initially formed graphene fiber as-released from the pipeline has a porous network structure (Figure S5b,c), which allows to spontaneously immobilize the embedded guest components during drying process. As demonstrated in Figure S10, the TiO_2 nanoparticles have been intercalated into the framework of graphene sheets by soaking the wet graphene fiber in commercial TiO_2 (AEROXIDE P25) aqueous suspension (10 mg/mL) for 20 min with slight stir. After drying and annealing at 400 °C for 30 min, the TiO_2/graphene fiber (~8 wt%) exhibits a fast photocurrent response with good repeatability (Figure 4c). The strong photocurrent response indicates a direct electron/hole injection between the TiO_2 particles and graphene sheets through photoexcitation of TiO_2,[29] suggesting the significant applications in optoelectronic systems such as photodetectors, photocatalysts and photovoltaic cells. In spite of the absence of optimizing the fabrication process in this primary study, Fe_3O_4- and TiO_2/graphene fibers are still flexible and have a half of the tensile strength of neat graphene fibers.

Large scale preparation of graphene fibers can be done by scaling up the pipelines and ovens, and continuous production of graphene fibers by setup of a thermal-flow circulatory pipeline system is underway. The strong but low-weight graphene fibers with appropriate functionalization, as well as the controllable shaping and stitchability, could be integrated into flexible and hierarchically engineered structures for a variety of specific applications such as smart clothing and electronic textiles.

Experimental Section

For preparation of graphene fibers, 8 mg/mL aqueous GO suspension [30] was injected into the glass pipeline with a 0.4 mm inner diameter by use of a syringe (Figure S1), which was then baked in an oven at 230 °C for 2 h after sealing up the two ends of the pipeline. Finally, a graphene fiber matching the pipe geometry was produced. The preformed graphene fiber was released from the pipeline by flow of N_2, which had a diameter of about 150 μm in this wet state and was hold by glass slides for drying in air (Figure S4). The dried graphene fiber almost remains the length but its diameter reduced to ~35 μm due to the water loss. The as-prepaed graphene fiber is very flexible, and can be woven to the meshwork-like and cloth-like structures by hands. The graphene fiber network can also be embedded into the polydimethylsiloxane (PDMS) matrix by casting a mixed and degassed PDMS prepolymer (Dow Corning, with a ratio of base to cross-linker of 10:1 by mass) on graphene fiber meshes, followed by curing at 60 °C for several hours.

Magnetic Fe_3O_4/graphene fibers were prepared by mixing Fe_3O_4 nanoparticles (20 nm, Aladdin Chemistry Co. Ltd) with 8 mg/mL GO suspension under ultrasonication (weight ratio of Fe_3O_4/GO = 1:10),

Adv. Mater. **2012**,
DOI: 10.1002/adma.201200170

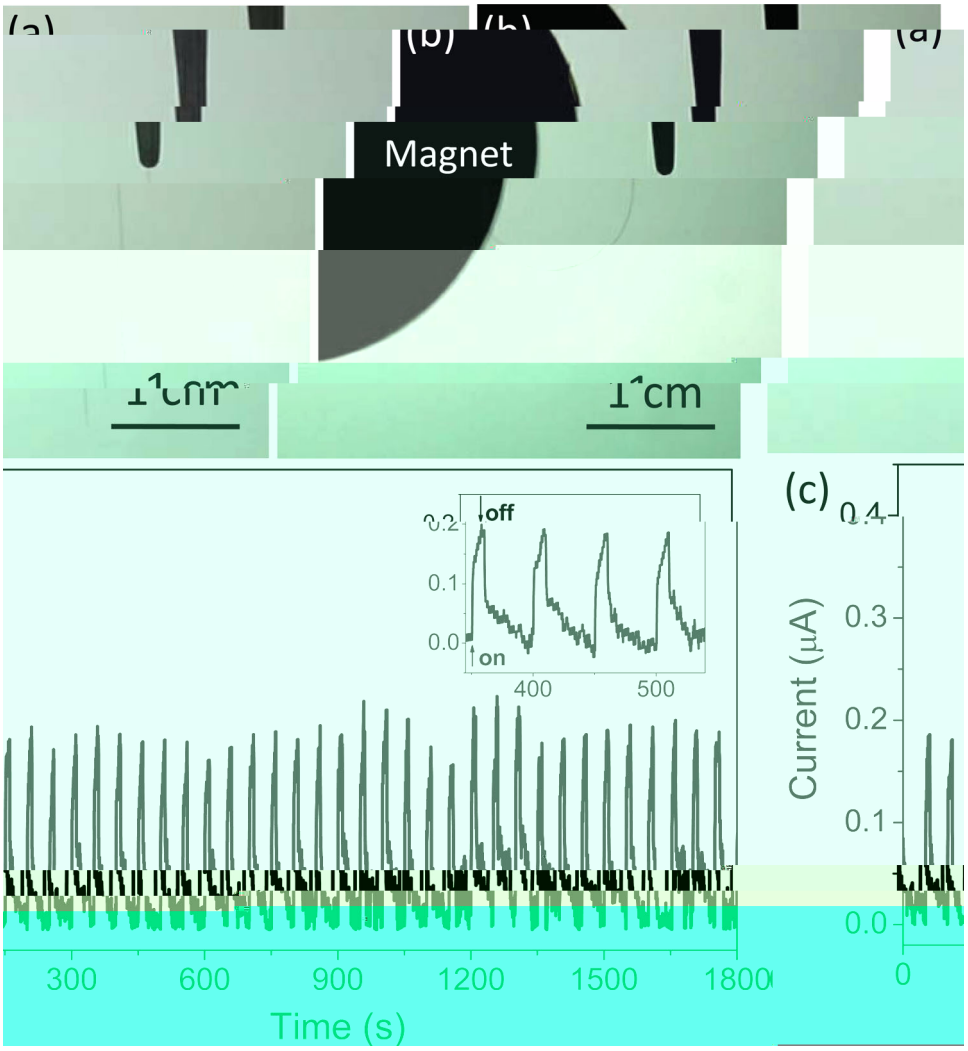

Figure 4. Magnetic and photoelectric response of functional graphene fibers. (a,b) the straight Fe_3O_4/graphene fiber and the Fe_3O_4/graphene fiber attracted to the magnet. (c) A typical photocurrent response for an 8 wt% TiO_2 immobilized graphene fiber upon exposure to on/off light at room temperature. The inset shows an enlarged view for a small portion of the photocurrent response curve. The sample length is 1 cm.

followed by hydrothermal process within pipelines as mentioned above for in-situ incorporation of Fe_3O_4 nanoparticles into the interlayers of graphene sheets. The dry Fe_3O_4/graphene fiber with good mechanical flexibility possesses a sensitive magnetic response.

TiO_2 nanoparticles (21 nm in diameter) were intercalated into the framework of graphene sheets by soaking the wet graphene fiber in commercial AEROXIDE TiO_2 P25 (Degussa Co., Germany) aqueous suspension (10 mg/mL) for 20 min with slight stir. The TiO_2 embedded wet graphene fiber (~8 wt%) was dried in air and annealed at 400 °C for 30 min under N_2 prior to the photocurrent measurement. The photocurrent response of TiO_2/graphene fiber was measured by applying a bias of 0.1 V to the fiber with about 1 cm electrode distance, while the current was recorded by CHI 660D electrochemical workstation upon exposure to a daylight lamp (100 W). More characterization details are included in Supporting Information.

Supporting Information

Supporting Information is available from the Wiley Online Library or from the author.

Acknowledgements

We thank the financial support from National Basic Research Program of China (2011CB013000) and NSFC (21004006, 21174019).

Received: January 13, 2012
Published online:

[1] A. B. Dalton, S. Collins, E. Muñoz, J. M. Razal, V. H. Ebron, J. P. Ferraris, J. N. Coleman, B. G. Kim, R. H. Baughman, *Nature* **2003**, *423*, 703.
[2] L. M. Ericson, H. Fan, H. Peng, V. A. Davis, W. Zhou, J. Sulpizio, Y. Wang, R. Booker, J. Vavro, C. Guthy, A. N. G. Parra-Vasquez, M. J. Kim, S. Ramesh, R. K. Saini, C. Kittrell, G. Lavin, H. Schmidt, W. W. Adams, W. E. Billups, M. Pasquali, W. F. Hwang, R. H. Hauge, J. E. Fischer, R. E. Smalley, *Science* **2004**, *305*, 1447.
[3] B. Vigolo, A. Pénicaud, C. Coulon, C. Sauder, R. Pailler, C. Journet, P. Bernier, P. Poulin, *Science* **2000**, *290*, 1331.
[4] V. A. Davis, A. N. G. Parra-Vasquez, M. J. Green, P. K. Rai, N. Behabtu, V. Prieto, R. D. Booker, J. Schmidt, E. Kesselman,

W. Zhou, H. Fan, W. W. Adams, R. H. Hauge, J. E. Fischer, Y. Cohen, Y. Talmon, R. E. Smalley, M. Pasquali, *Nat. Nanotechnol.* **2009**, *4*, 830.
[5] K. Jiang, Q. Li, S. Fan, *Nature* **2002**, *419*, 801.
[6] Y. Li, I. A. Kinloch, A. H. Windle, *Science* **2004**, *304*, 276.
[7] M. Zhang, K. R. Atkinson, R. H. Baughman, *Science* **2004**, *306*, 1358.
[8] X. B. Zhang, K. L. Jiang, C. Feng, P. Liu, L. Zhang, J. Kong, T. Zhang, Q. Li, S. S. Fan, *Adv. Mater.* **2006**, *18*
[17] H. Chen, M. B. Müller, K. J. Gilmore, G. G. Wallace, D. Li, *Adv. Mater.* **2008**, *20*, 3557.
[18] D. Li, M. B. Müller, S. Gilje, R. B. Kaner, G. G. Wallace, *Nat. Nanotechnol.* **2008**, *3*, 101.
[19] G. Eda, G. Fanchini, M. Chhowalla, *Nat. Nanotechnol.* **2008**, *3*, 270.
[20] X. L. Li, G. Zhang, X. Bai, X. Sun, X. Wang, E. Wang, H. Dai, *Nat. Nanotechnol.* **2008**, *3*, 538.
[21] Y. Xu, K. Sheng, C. Li, G. Shi, *ACS Nano* **2010**, *4*, 4324.
[22] S. H. Lee, H. W. Kim, J. O. Hwang, W. J. Lee, J. Kwon, C. W. Bielawski, R. S. Ruoff, S. O. Kim, *Angew. Chem. Int. Ed.* **2010**, *49*, 10084.
[23] X. Li, T. Zhao, K. Wang, Y. Yang, J. Wei, F. Kang, D. Wu, H. Zhu, *Langmuir* **2011**, *27*,12164.
[24] Z. Xu, C. Gao, *Nat. Commun.* **2011**, doi: 10.1038/ ncomms1583.
[25] http://efie.net/efficiency/a-new-way-to-make-carbon-fiber/
[26] H. H. Gommans, J. W. Alldredge, H. Tashiro, J. Park, J. Magnuson, and A. G. Rinzler, *J. Appl. Phys.* **2000**, *88*, 2509.
[27] G. S. Duesberg, I. Loa, M. Burghard, K. Syassen, S. Roth, *Phys. Rev. Lett.* **2000**, *85*, 5436.
[28] J. A. Rogers, T. Someya, Y. G. Huang, *Science* **2010**, *327*, 1603.
[29] Y. D. Yang, L. T. Qu, L. M. Dai, T. S. Kang, M. Durstock, *Adv. Mater.* **2007**, *19*, 1239.
[30] Y. X. Xu, H. Bai, G. W. Lu, C. Li, G. Q. Shi, *J. Am. Chem. Soc.* **2008**, *130*, 5856.